Journal of Applied Fluid Mechanics, Vol. 9, No. 2, pp. 809-816, 2016.
Available online at www.jafmonline.net, ISSN 1735-3572, EISSN 1735-3645.
DOI: 10.18869/acadpub.jafm.68.225.24644

Characteristics of Homogeneous-Heterogeneous Reactions and Melting Heat Transfer in the Stagnation Point flow of Jeffrey Fluid

T. Hayat[1,2] , M. Farooq[1,2] and A. Alsaedi[2]

[1]Department of Mathematics, Quaid-I-Azam University 45320, Islamabad 44000, Pakistan.
[2]Nonlinear Analysis and Applied Mathematics (NAAM) Research Group, *Department of Mathematics, Faculty of Science, King Abdulaziz University, P. O. Box* 80257, *Jeddah* 21589, *Saudi Arabia*

†Corresponding Author Email: hfarooq99@yahoo.com

(Received January 29, 2015; accepted May 6, 2015)

ABSTRACT

This work focuses on melting heat transfer in the stagnation point flow of Jeffrey fluid past an impermeable stretching cylinder with homogeneous-heterogeneous reactions. Characteristics of magnetohydrodynamic flow are explored in presence of heat generation/absorption. Diffusion coefficients of species A and B are taken of the same size. Heat released during chemical reaction is negligible. A system of ordinary differential equations is obtained by using suitable transformations. Convergent series solutions are derived. Impacts of various pertinent parameters on the velocity, temperature and concentration distributions are discussed. Numerical values of skin friction coefficient and Nusselt number are computed and analyzed. Present results are compared with the previous published data.

Keywords: Stagnation point flow; Melting heat transfer; Homogeneous-Heterogeneous reactions; Jeffrey fluid.

1. INTRODUCTION

Scientists and researchers are still interested in exploring the behaviors and characteristics of non-Newtonian fluids. Such inspiration is due to numerous applications of non-Newtonian fluids in physiology, pharmaceuticals, fiber technology, coating of wires, food products, crystal growth etc. Characteristics of non-Newtonian fluids cannot be analyzed by a single constitutive relationship. Therefore various models are proposed for the non-Newtonain fluids. Generally the non-Newtonian fluids are categorized into three main types i.e., (i) Differential type (ii) Rate type and (iii) Integral type. Rate type fluids describe the behavior of relaxation and retardation times. Maxwell fluid is a subclass of rate type material which exhibits the behavior of relaxation time only. This model does not present the behavior of retardation time. Thus Jeffrey fluid model (Turkyilmazoglu and Pop (2013), Hayat *et al*. (2015), Ellahi *et al*. (2014), Dalir *et al*. (2015), Hayat *et al*. (2013)) is proposed to fill this void. Jeffrey fluid model characterizes the linear viscoelastic properties of fluids which has wide spread applications in the polymer industries.

Recently the phenomenon of melting heat transfer has received the attention of researchers and scientists due to their widespread applications in the advanced technological and industrial processes. The melting of soil, the freezing of soil around the heat exchanger coils of a ground based pump, melting of permafrost, magma solidification, thawing of frozen grounds, the freeze treatment of sewage, the preparation of semiconductor material, the casting and welding of a manufacturing process are the important applications of melting phenomenon (Rahman *et al*. (2013)). Robert (1985) for the first time described melting phenomenon of ice slab placed in a hot stream of air. Hayat *et al*. (2013) presented boundary layer stagnation point flow of melting heat transfer in Powell-Eyring fluid. Radiative melting heat transfer in the magnetohydrodynamic flow over a moving surface was investigated by Das (2014). Characteristics of melting heat transfer in the flow of Maxwell fluid with double diffusive convection were explored by Hayat *et al*. (2014). Awais *et al*. (2014) examined melting heat transfer in the boundary layer stagnation point flow of Burgers' fluid. Prasad *et al*. (2014) analyzed melting heat transfer and mixed convection boundary layer flow of non-Newtonian fluid saturated by porous medium over a vertical plate.

Chemical reactions in the natural processes involve

both homogeneous and heterogeneous reactions. Also there exist some of the reactions which have less ability to proceed quickly or not at all, except in the presence of a catalyst. The interaction between the homogeneous and heterogeneous reactions are very complex involving the production and consumption of reactant species at different rates both within the fluid and on the catalyst surface such as reactions occurring in combustion, catalysis and biochemical systems. Merkin (1996) explored the properties of homogeneous heterogeneous reactions in the boundary layer flow for isothermal model. Characteristics of homogeneous-heterogeneous reactions in micropolar fluid embedded in porous medium past a stretching/shrinking sheet were analyzed by Shaw *et al.* (2013). The analysis of homogeneous-heterogeneous reactions in flow of nanofluid past a permeable stretching sheet was examined by Kameswaran *et al.* (2013).

The objective of the present investigations is to explore the characteristics of homogeneous heterogeneous reactions in the stagnation point flow of Jeffrey fluid past a cylinder with melting heat transfer. Behavior of heat transfer is modeled and analyzed with heat generation/absorption. Diffusion coefficients of both species are assumed equal. Convergent series solutions are computed via homotopy analysis method (Liao (2012), Turkyilmazoglu (2012), Beg *et al.* (2012), Shehzad *et al.* (2014), Abbasbandy (2013), Hayat *et al.* (2015)). Behavior of various pertinent parameters on the skin friction coefficient and Nusselt number are presented numerically. Present results for skin friction coefficient and Nusselt number are compared with previous published work in limiting sense. Excellent agreement between the results is obtained.

2. MATHEMATICAL FORMULATION

We consider the steady melting heat transfer in the stagnation point flow of Jeffrey fluid by an impermeable stretching cylinder. Magnetohydrodynamic flow analysis is explored with homogeneous-heterogeneous reactions and heat generation/absorption. Cylindrical coordinates are chosen in such a way that X-axis is along the axial direction of cylinder while r-axis is normal to it. Stretching velocity of the cylinder is originated by applying two forces which are equal in magnitude but opposite in direction such that origin is kept fixed. Ambient temperature T_∞ is assumed greater than the melting surface temperature T_m. The heat released by the reaction is assumed negligible. The homogeneous reaction for cubic autocatalysis can be expressed as follows:

$$\mathbf{A}+2\mathbf{B}\rightarrow 3\mathbf{B},\quad \text{rate}=k_1ab^2, \tag{1}$$

while first-order isothermal reaction on the catalyst surface is presented in the form

$$\mathbf{A}\rightarrow \mathbf{B},\quad \text{rate}=k_s a. \tag{2}$$

Here a and b are the concentrations of chemical species **A** and **B** while k_1 and k_s are the rate constants. These equations of reactions ensure that the reaction rate is zero in the external flow and at the outer edge of the boundary layer. Using the boundary layer approximations ($o(x)=o(u)=o(1)$, $o(r)=o(v)=o(\delta)$), the conservation laws of mass, linear momentum and energy take the forms:

$$\frac{\partial(rv)}{\partial r}+\frac{\partial(ru)}{\partial x}=0, \tag{3}$$

$$u\frac{\partial u}{\partial x}+v\frac{\partial u}{\partial r}=U_e\frac{dU_e}{dx}+\frac{\upsilon}{1+\lambda_1}\left[\frac{1}{r}\frac{\partial u}{\partial r}+\frac{\partial^2 u}{\partial r^2}+\lambda_2\left(\begin{array}{l}\frac{v}{r}\frac{\partial^2 u}{\partial r^2}+\frac{\partial v}{\partial r}\frac{\partial^2 u}{\partial r^2}+v\frac{\partial^3 u}{\partial r^3}+\\ \frac{u}{r}\frac{\partial^2 u}{\partial x\partial r}+\frac{\partial u}{\partial r}\frac{\partial^2 u}{\partial x\partial r}+v\frac{\partial^3 u}{\partial x\partial r^2}\end{array}\right)\right]-\frac{\sigma B_0^2}{\rho}(u-U_e), \tag{4}$$

$$u\frac{\partial T}{\partial x}+v\frac{\partial T}{\partial r}=\frac{k}{\rho c_p}\left(\frac{\partial^2 T}{\partial r^2}+\frac{1}{r}\frac{\partial T}{\partial r}\right)+\frac{Q_0}{\rho c_p}(T-T_m), \tag{5}$$

with

$$u\frac{\partial a}{\partial x}+v\frac{\partial a}{\partial r}=D_A\left(\frac{\partial^2 a}{\partial r^2}+\frac{1}{r}\frac{\partial a}{\partial r}\right)-k_1ab^2. \tag{6}$$

$$u\frac{\partial b}{\partial x}+v\frac{\partial b}{\partial r}=D_B\left(\frac{\partial^2 b}{\partial r^2}+\frac{1}{r}\frac{\partial b}{\partial r}\right)+k_1ab^2. \tag{7}$$

The subjected boundary conditions are

$$u=U_w(x)=\frac{U_0x}{l},\quad T=T_m,\ D_A\frac{\partial a}{\partial r}=k_s a,$$
$$D_B\frac{\partial b}{\partial r}=-k_s a \text{ at } r=R,$$
$$u\rightarrow U_e(x)=\frac{U_\infty x}{l},\quad T\rightarrow T_\infty,\quad a\rightarrow a_0,$$
$$b\rightarrow 0 \text{ as } r\rightarrow\infty,$$
$$k\left(\frac{\partial T}{\partial r}\right)_{r=R}=\rho\left[\lambda+c_s(T_m-T_0)\right]v(x,R). \tag{8}$$

In the above expressions u and v denote the velocity components in the axial and radial directions respectively, σ is the electrical conductivity, B_0 is the magnetic field, λ_1 is the ratio of relaxation to retardation times, λ_2 is the retardation time, R is the radius of cylinder, U_w and U_e are the stretching and free stream velocities respectively, ν is the kinematic viscosity, k is the thermal conductivity, ρ is the density, c_p is the specific heat, Q_0 is the heat generation/absorption coefficient, D_A and D_B are diffusion species coefficients of A and , T and T_m are the fluid and

melting surface temperatures, T_∞ is the ambient fluid temperature, l is the characteristic length, a_0 is the positive dimensional constant, λ is the latent heat of the fluid, T_0 and c_s are the temperature and heat capacity of the cylinder surface.

Considering the following transformations

$$\eta=\sqrt{\frac{U_0}{\nu l}}\left(\frac{r^2-R^2}{2R}\right),\qquad \psi=\sqrt{U_w\nu x}Rf(\eta),$$
$$u=\frac{U_0 x}{l}f'(\eta),$$
$$v=-\sqrt{\frac{\nu U_0}{l}}\frac{R}{r}f(\eta),\qquad \theta(\eta)=\frac{T-T_m}{T_\infty-T_m},\tag{9}$$
$$g(\eta)=\frac{a}{a_0},\ h(\eta)=\frac{b}{a_0},$$

incompressibility condition is satisfied automatically and Eqs. (4) to (7) are reduced to

$$(1+2\gamma\eta)f'''+(1+\lambda_1)\left(ff''-(f')^2\right)+2\gamma f''$$
$$+\gamma\beta\left(ff''-3ff'''\right)+(1+2\gamma\eta)\beta\left(f''^2-ff^{iv}\right)$$
$$+(1+\lambda_1)\left(A^2+Ha^2A\right)-(1+\lambda_1)Ha^2f'=0,\tag{10}$$

$$(1+2\gamma\eta)\theta''+2\gamma\theta'+\Pr f\theta'+\Pr\delta\theta=0,\tag{11}$$

$$\frac{1}{Sc}\left((1+2\gamma\eta)g''+2\gamma g'\right)+fg'-Kgh^2=0,\tag{12}$$

$$\frac{\delta_1}{Sc}\left((1+2\gamma\eta)h''+2\gamma h'\right)+fh'+Kgh^2=0,\tag{13}$$

with

$$f'(0)=1,\ \theta(0)=0,g'(0)=K_sg(0),$$
$$\delta_1h'(0)=-K_sg(0)$$
$$f'(\infty)\to A,\quad \theta(\infty)\to1,\tag{14}$$
$$g(\infty)\to1,\ \ h(\infty)\to0,$$

$$\Pr f(0)+M\theta'(0)=0,\tag{15}$$

where γ is the curvature parameter, A is the ratio of velocities, λ_1 is the ratio of relaxation to retardation times, β is the Deborah number in terms of retardation time, Ha is the Hartman number, $\Pr$ is the Prandtl number, δ is the heat generation/absorption parameter, K is the strength of homogeneous reaction parameter, K_s is the strength of heterogeneous reaction parameter, δ_1 is the ratio of mass diffusion coefficients, Sc is the Schmidt number and M is the melting parameter. These quantities are defined as follows:

$$\gamma=\left(\frac{\nu l}{U_0R^2}\right)^{1/2},\ \Pr=\frac{\mu c_p}{k},\ \beta=\frac{\lambda_2U_0}{l},$$
$$A=\frac{U_\infty}{U_0},\quad Sc=\frac{\nu}{D_A},\ K=\frac{k_1a_0^2l}{U_w},$$
$$\delta_1=\frac{D_B}{D_A},\ K_s=\frac{k_s}{D_A}\sqrt{\frac{\nu l}{U_0}},\ M=\frac{c_p(T_\infty-T_m)}{\lambda+c_s(T_m-T_0)},\ \delta=\frac{Q_0l}{U_0\rho c_p}.\tag{16}$$

Here it is assumed that diffusion coefficients of chemical species **A** and **B** to be of a comparable size. This argument provides us to make further assumption that the diffusion coefficients D_A and D_B are equal i.e. $\delta_1=1$ and thus (Kameswaran *et al*. (2013)):

$$g(\eta)+h(\eta)=1.\tag{17}$$

Now Eqs. (12) and (13) yield

$$\frac{1}{Sc}\left((1+2\gamma\eta)g''+2\gamma g'\right)+fg'-Kg(1-g)^2=0,\tag{18}$$

with the boundary conditions

$$g'(0)=K_sg(0),\quad g(\eta)\to1\quad\text{as}\quad\eta\to\infty.\tag{19}$$

Skin friction coefficient and local Nusselt number are defined as follows:

$$C_f=\frac{\tau_w}{\rho U_w^2},\qquad Nu_x=\frac{xq_w}{k(T_\infty-T_m)},$$
$$\tau_w=\frac{\mu}{1+\lambda_1}\left[\left(\frac{\partial u}{\partial r}\right)+\lambda_2\left[v\frac{\partial^2u}{\partial r^2}+u\frac{\partial^2u}{\partial x\partial r}\right]\right]_{r=R},\tag{20}$$

$$q_w=-\kappa\left(\frac{\partial T}{\partial r}\right)_{r=R}.\tag{21}$$

Dimensionless skin friction coefficient and local Nusselt number are

$$C_f\,\mathrm{Re}_x^{1/2}=\frac{1}{(1+\lambda_1)}\begin{pmatrix}f''(0)-\beta f(0)f'''(0)\\-\beta\gamma f(0)f''(0)\\+\beta f'(0)f''(0)\end{pmatrix},$$
$$Nu_x\,\mathrm{Re}_x^{-1/2}=-\theta'(0),\tag{22}$$

where $\mathrm{Re}_x=U_wx/\nu$ is the Reynolds number.

3. HOMOTOPIC SOLUTIONS

Homotopy analysis method was first proposed by Liao (2012) in 1992 which is used to obtain the solutions of highly nonlinear problems. It provides us a great freedom to choose the initial guesses and linear operators for the construction of series solutions. Thus we have

$$f_0(\eta)=A\eta+(1-A)\left(1-\exp(-\eta)\right)-\frac{M}{\Pr},$$
$$\theta_0(\eta)=1-\exp(-\eta),$$
$$g_0(\eta)=1-\frac{1}{2}\exp(-K_s\eta),\tag{23}$$

$$\mathbf{L}_f(f)=\frac{d^3f}{d\eta^3}-\frac{df}{d\eta},\quad \mathbf{L}_\theta(\theta)=\frac{d^2\theta}{d\eta^2}-\theta,$$

$$\mathbf{L}_g(g)=\frac{d^2g}{d\eta^2}-g, \tag{24}$$

with

$$\mathbf{L}_f\left[A_1+A_2\exp(\eta)+A_3\exp(-\eta)\right]=0, \tag{25}$$

$$\mathbf{L}_\theta\left[A_4\exp(\eta)+A_5\exp(-\eta)\right]=0, \tag{26}$$

$$\mathbf{L}_g\left[A_6\exp(\eta)+A_7\exp(-\eta)\right]=0, \tag{27}$$

where A_i $(i=1,2,...,7)$ are the arbitrary constants. The zeroth and mth order deformation problems are:

Convergence analysis

Homotopy analysis technique provides us great freedom and an easy way to adjust and control the convergence region of the series solutions. Convergence region is the region parallel to $\hbar$ -axis. Therefore we have plotted the $\hbar$ -curves in the Figs. 1-2. It is found that the admissible ranges of the auxiliary parameters $\hbar_f$, $\hbar_\theta$ and $\hbar_g$ are $-1.3\le\hbar_f\le-0.8$, $-1.2\le\hbar_\theta\le-0.8$ and $-1.15\le\hbar_g\le-0.6$.

4. DISCUSSION

The main focus of this section is to analyze the characteristics of various parameters on the axial velocity, temperature and concentration distributions. Characteristics of ratio parameter A on the velocity distribution are illustrated in Fig. 3. It is concluded that velocity profile increases for $A>1$ and for $A<1$ the boundary layer thickness has opposite effects. It is also examined that there is no formation of boundary layer for $A=1$ i.e., fluid and cylinder move with the same velocity. Fig. 4 shows the behavior of Deborah number β on the velocity distribution. Here we analyzed that velocity distribution enhances for larger values of Deborah number. Higher values of Deborah number corresponds to higher characteristics of elasticity which is responsible in enhancement of the velocity profile. Influence of melting parameter M on the velocity distribution is displayed in Fig. 5. It is noted that velocity distribution is higher for larger values of melting parameter. As a result of melting, more heat transfers from the heated fluid to the melting surface which corresponds to higher convection flow. Therefore velocity profile increases. Effect of curvature parameter γ on the velocity profile is sketched in Fig. 6. Velocity profile decreases near the surface of cylinder while it increases gradually far away from the surface.

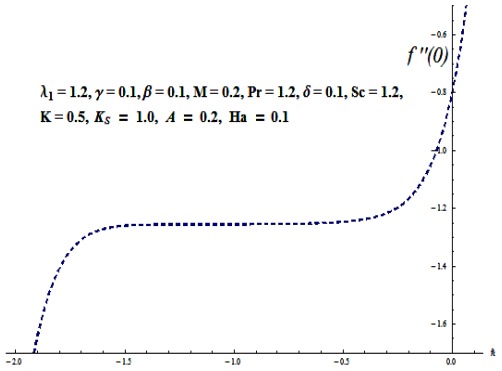

Fig. 1. $\hbar$ -curve for f.

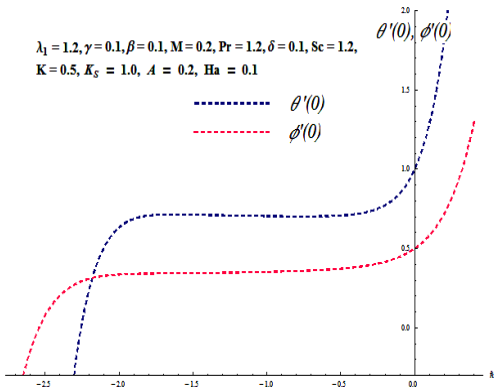

Fig. 2. $\hbar$ -curves for θ and ϕ.

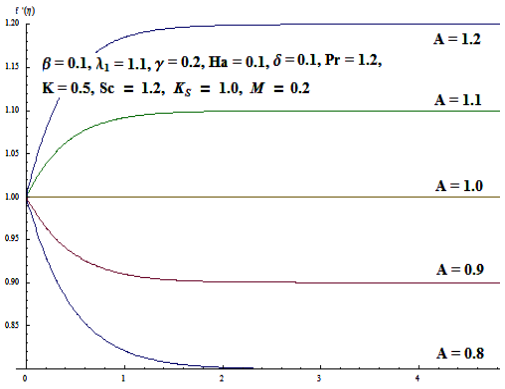

Fig. 3. Effect of A on f'.

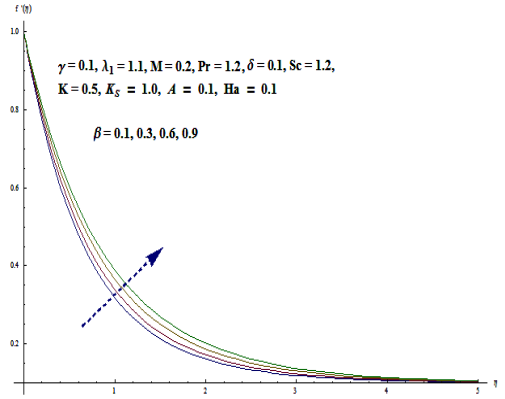

Fig. 4. Effect of β on f'.

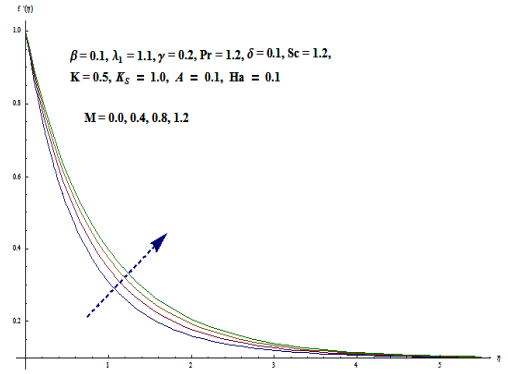

Fig. 5. Effect of M on f'.

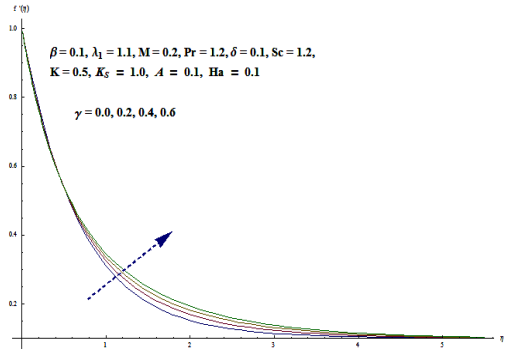

Fig. 6. Effect of γ on f'.

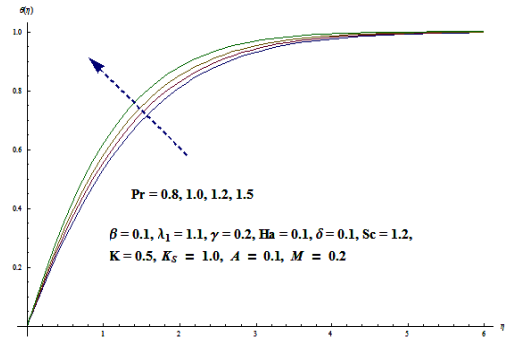

Fig. 7. Effect of Pr on θ.

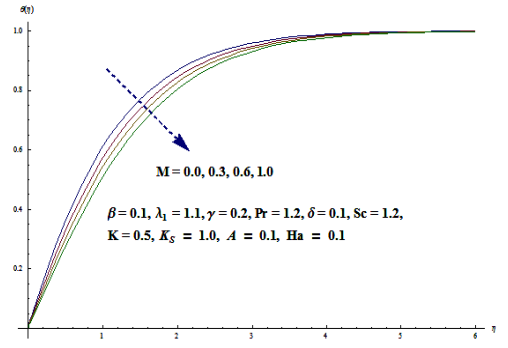

Fig. 8. Effect of M on θ.

In fact for higher values of curvature parameter, the radius of cylinder decreases which reduces contact area of the cylinder with the fluid. Therefore velocity profile increases. Characteristics of Prandtl number Pr on temperature distribution is sketched in Fig. 7. It is shown that temperature distribution increases for larger values of Prandtl number. Prandtl number is the ratio of momentum diffusivity to thermal diffusivity. Higher Prandtl number corresponds to lower thermal diffusivity. Hence less heat is transferred from heated fluid to the melting surface and as a result the temperature distribution remains higher. Behavior of melting parameter M on the temperature distribution is shown in Fig. 8. Temperature distribution is higher for small values of melting parameter. Further higher values of melting parameter result in enhancement of thermal boundary layer thickness. It is due to fact that more heat transfers from heated fluid to the melting surface due to higher melting parameter which results in the reduction of temperature distribution. Influence of heat generation/absorption on temperature profile is presented in Fig. 9. Temperature profile decreases with an increase in heat absorption parameter $\delta < 0$ while it increases with an increase in heat generation parameter $\delta > 0$. It is also noted that thermal boundary layer thickness has opposite effects for heat generation and absorption parameters. In case of heat generation more heat produced which is responsible for enhancement of temperature profile. Effect of curvature parameter γ on temperature profile is sketched in Fig. 10. It is found that temperature profile increases near the surface of cylinder while it decreases away from the surface. For higher values of curvature parameter, the radius of cylinder decreases which offers less resistance. Therefore temperature near the surface of cylinder increases. Influence of strength of homogeneous reaction K on concentration distribution is sketched in Fig. 11. Concentration profile decreases while boundary layer thickness increases for higher values of strength of homogeneous reaction parameter. Behavior of strength of heterogeneous reaction parameter K_S on the concentration distribution is analyzed in Fig. 12. Concentration distribution decreases near the surface of cylinder and it increases away from the surface for higher values of K_S.

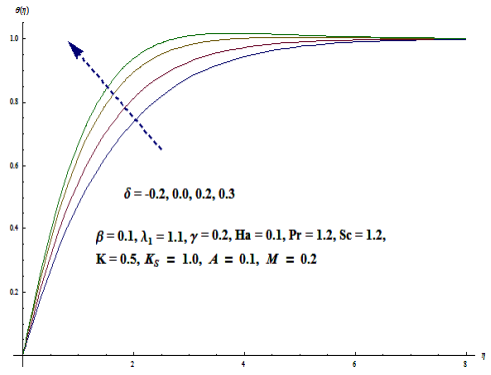

Fig. 9. Effect of δ on θ.

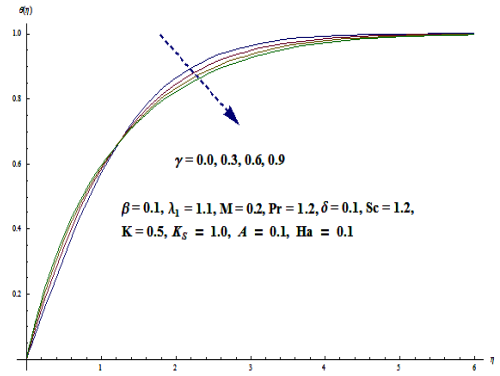

Fig. 10. Effect of γ on θ.

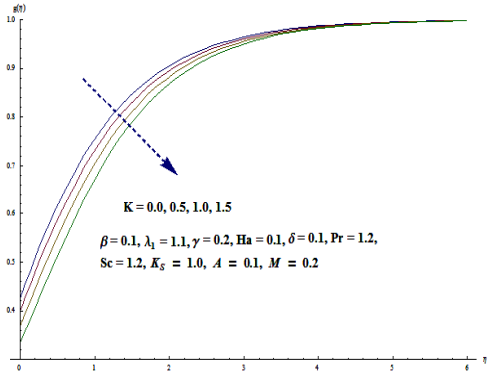

Fig. 11. Effect of K on g.

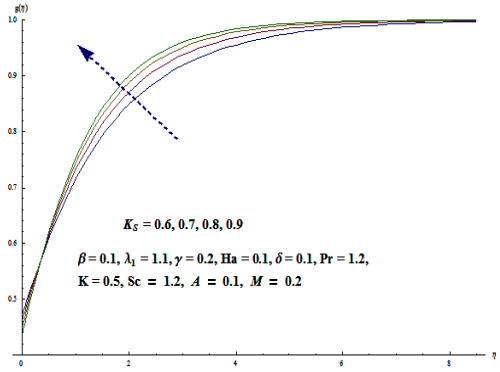

Fig. 12. Effect of K_s on g.

Table 1 shows the convergence analysis of the series solutions for momentum, energy and concentration equations. It is concluded that 21th order of approximations are sufficient for convergence analysis of momentum equation while 25th order of approximations are enough for energy and concentration equations. Table 2 presents behavior of various parameters on skin friction coefficient. Higher values of γ, β and Ha result in enhancement of skin friction coefficient while it decreases for larger values of A, λ_1 and M. Table 3 shows the characteristics of various pertinent parameters on Nusselt number. It is noted that Nusselt number increases for higher values of γ, Pr, δ and A while it decreases with an increase in M and Ha. Tables 4 and 5 represent the comparison of skin friction coefficient and Nusselt number with the previous published work of Awais *et al*. (2013), Mahapatra and Gupta (2002), Pop *et al*. (2004) and Sharma and Singh (2009). The results show excellent agreement.

Table 1 Convergence of series solutions for different order of approximations when $\lambda_1 = 1.2$, $\gamma = 0.1$, $\beta = 0.1$, $M = 0.2$, $Pr = 1.2$, $\delta = 0.1$, $Sc = 1.2$, $K = 0.5$, $K_s = 1.0$, $A = 0.2$ and $Ha = 0.1$

Order of approximations	-f″(0)	θ′(0)	g′(0)
1	1.0015	0.8856	0.4638
5	1.2192	0.7345	0.3973
10	1.2487	0.7064	0.3702
15	1.2536	0.7042	0.3586
21	1.2548	0.7081	0.3513
25	1.2548	0.7096	0.3496
30	1.2548	0.7096	0.3496

Table 2 Numerical values of skin friction coefficient for different parameters when $Pr = 1.2$ and $\delta = 0.1$

A	λ1	γ	β	M	Ha	$-C_f\,\mathrm{Re}_x^{1/2}$
0.0	1.2	0.2	0.1	0.2	0.1	0.6850
0.1						0.6647
0.3						0.5848
0.1	1.0					0.7015
	1.2					0.6647
	1.5					0.6184
	1.2	0.0				0.6359
		0.2				0.6647
		0.5				0.7069
		0.2	0.1			0.6647
			0.2			0.6936
			0.3			0.7226
			0.1	0.0		0.7248
				0.2		0.6647
				0.5		0.6003
				0.2	0.0	0.6617
					0.1	0.6447
					0.4	0.7080

5. CLOSING REMARKS

In the presented analysis, we have explored the characteristics of melting heat transfer in the MHD stagnation point flow of Jeffrey fluid induced by an impermeable stretching cylinder with homogeneous-heterogeneous chemical reactions. Heat transfer characteristics are modeled and analyzed with heat generation/absorption. The key points are summarized as follows:

- Melting parameter results in enhancement of velocity and associated boundary layer thickness.

- Velocity distribution decreases near the surface of cylinder while it increases away from the surface for higher values of curvature parameter.
- Temperature distribution decreases for higher values of melting parameter while thermal boundary layer thickness increases.
- Concentration distribution decreases for larger values of strength of homogeneous reaction K .
- Higher values of strength of heterogeneous reaction K_s result in enhancement of concentration profile.

Table 3 Numerical values of Nusselt number for different parameters when $\lambda_1 = 1.2$ and $\beta = 0.1$

γ	Pr	δ	M	Ha	A	-θ′(0)
0.0	1.2	0.1	0.2	0.1	0.1	0.6387
0.2						0.7434
0.5						0.8795
0.2	0.8					0.6238
	1.2					0.7434
	1.4					0.7942
	1.2	0.0				0.6603
		0.1				0.7434
		0.3				0.8591
		0.1	0.0			0.8277
			0.2			0.7434
			0.4			0.6765
			0.2	0.0		0.7438
				0.1		0.7434
				0.3		0.7399
				0.1	0.0	0.7331
					0.1	0.7434
					0.4	0.7814

Table 4 Comparison of skin friction coefficient ($f''(0)$) with Mahapatra and Gupta (2002), Pop *et al*. (2004) and Sharma and Singh (2009) for various values of A when $\gamma = 0, \lambda_1 = 0$, $\beta = 0$, $Ha = 0$, $\delta = 0$ and $M = 0$

A	Mahapatra and Gupta (2002)	Pop *et al*. (2004)	Sharma and Singh (2009)	Present results
0.1	-0.9694	-0.9694	-0.969386	-0.96939
0.2	-0.9181	-0.9181	-0.9181069	-0.91811
0.5	-0.6673	-0.6673	-0.667263	-0.66726
0.7				-0.43346
0.8				-0.29929
0.9				-0.15458
1.0				0.00000

ACKNOWLEDGMENT

The first two authors acknowledge the financial support of Higher Education Commission (HEC) of Pakistan.

Table 5 Comparison of Nusselt number ($-\theta'(0)$) with Mahapatra and Gupta (2002) and Awais *et al*. (2014) for various values of A and Pr when $\gamma = 0, \lambda_1 = 0$, $\beta = 0$, $Ha = 0$, $\delta = 0$ and $M = 0$

Pr	A	Mahapatra and Gupta (2002)	Awais *et al*. (2014)	Present results
1.0	0.1	0.603	0.602156	0.6022
	0.5	0.692	0.692460	0.6926
1.5	0.1	0.777	0.776802	0.7768
	0.5	0.863	0.864771	0.8646

REFERENCES

Abbasbandy, S., M. S. Hashemi and I. Hashim (2013). On convergence of homotopy analysis method and its application to fractional integro-differential equations. *Quaestiones Mathematicae* 36, 93-105.

Awais, M., T. Hayat and A. Alsaedi (2014). Investigation of heat transfer in flow of Burgers' fluid during a melting process. *J. Egyp. Math. Soc*. (In press).

Beg, O. A., M. M. Rashidi, T. A. Beg and M. Asadi (2012). Homotopy analysis of transient magneto-Bio-fluid dynamics of micropolar squeeze film in a porous medium: A model for magneto-Bio-Rheological lubrication. *Journal of Mechanics in Medicine and Biology*. 12**,** 1250051.

Dalir, N., M. Dehsara and S. S. Nourazar (2015). Entropy analysis for magnetohydrodynamic flow and heat transfer of a Jeffrey nanofluid over a stretching sheet. *Energy* 79, 351-362.

Das, K. (2014). Radiation and melting effects on MHD boundary layer flow over a moving surface. *Ain Shams Eng*. J. 5, 1207-1214.

Ellahi, R., S. U. Rahman and S. Nadeem (2014). Blood flow of Jeffrey fluid in a catherized tapered artery with the suspension of nanoparticles. *Phys. Letter A* 378, 2973-2980.

Hayat, T., S. Asad, M. Mustafa and A. Alsaedi (2015). MHD stagnation-point flow of Jeffrey fluid over a convectively heated stretching sheet. *Computers & Fluids* 108, 179-185.

Hayat, T., M. Farooq, A. Alsaedi and Z. Iqbal (2013). Melting heat transfer in the stagantion point flow of Powell-Eyring fluid. J. Thermophys. *Heat Transfer* 27, 761-766.

Hayat, T., M. Farooq and A. Alsaedi (2014). Melting heat transfer in the stagnation point flow of Maxwell fluid with double diffusive convection. *Int. J. Numer. Methods Heat Fluid Flow* 24, 760-774.

Hayat, T., M. Hussain, A. Alsaedi, S. A. Shehzad and G. Q. Chen (2015). Flow of Power-law nanofluid over a stretching surface with Newtonian heating. *J. Applied Fluid Mech.* 8, 273-280.

Hayat, T., A. Qayyum, F. Alsaadi, M. Awais and A. M. Dobaie (2013). Thermal radiation effects in squeezing flow of a Jeffrey fluid. *Eur. Phys. J. Plus* 128, 85.

Kameswaran, P. K., S. Shaw, P. Sibanda and P. V. S. N. Murthy (2013). Homogeneous-heterogeneous reactions in a nanofluid flow due to a porous stretching sheet. *Int. J. Heat Mass Transfer* 57, 465-472.

Liao, S. J. (2012). *Homotopy analysis method in non-linear differential equations*. Springer and Higher Education Press, Heidelberg

Mahapatra, T. R. and A. Gupta (2002). Heat transfer in stagnation-point flow towards a stretching sheet. *Heat Mass Trans*. 38, 517-521.

Merkin, J. H. (1996). A model for isothermal homogeneous-heterogeneous reactions in boundary-layer flow. *Math. Computer Model*. 24, 125-136.

Pop, S., T. Grosan and I. Pop (2004). Radiation effects on the flow near the stagnation point of a stretching sheet. *Technische Mechanik* 25, 100-106.

Prasad, J. S. R., K. Hemalatha and B. D. C. N. Prasad (2014). Mixed convection flow from vertical plate embedded in non-Newtonian fluid saturated non-Darcy porous medium with thermal dispersion-radiation and melting effects. *J. Appl. Fluid Mech*. 7, 385-394.

Rahman, R. G. A., M. M. Khadar and A. M. Megahed (2013). Melting phenomenon in magnetohydrodynamics steady flow and heat transfer over a moving surface in the presence of thermal radiation. *Chin. Phys. B* 22, 030202.

Roberts, L. (1985). On the melting of a semi-infinite body of ice placed in a hot stream of air. *J. Fluid Mech*. 4, 505-528.

Sharma, P. and G. Singh (2009). Effects of variable thermal conductivity and heat source/sink on MHD flow near a stagnation point on a linearly stretching sheet. *J. Appl. Fluid Mech*. 2, 13-21.

Shaw, S., P. K. Kameswaran and P. Sibanda (2013). Homogeneous-heterogeneous reactions in micropolar fluid flow from a permeable stretching or shrinking sheet in a porous medium. Boundary value Problems 2013, 77.

Shehzad, S. A., T. Hayat, M. S. Alhuthali and S. Asghar (2014). MHD three-dimensional flow of Jeffrey fluid with Newtonian heating. *J. Central South Univ*. 21, 1428-1433.

Turkyilmazoglu, M. (2012). Solution of the Thomas-Fermi equation with a convergent approach. Commun. *Nonlinear Sci. Numer. Simulat* 17, 4097-4103.

Turkyilmazoglu, M. and I. Pop (2013). Exact analytical solutions for the flow and heat transfer near the stagnation point on a stretching / shrinking sheet in a Jeffrey fluid. *Int. J. Heat Mass Transfer* 57, 82-88.